Inhibition of complement factor C5a or C5aR for cholesterol crystal embolism–related vascular thrombosis with microvascular injury and its consequences

OPEN

Danyang Zhao[1], Chao Han[1,2], Elmina Mammadova-Bach[1,2], Kanako Watanabe-Kusunoki[1,3], Tamisa Seeko Bandeira Honda[1], Yihong Li[4], Chenyu Li[1], Qiubo Li[1], Hao Long[1,5,6], Lyuben Lyubenov[1], Chongxu Shi[1,7], Donato Santovito[8,9], Christian Weber[8,9,10,11], Peter Boor[12,13], Patrick Droste[12,13], Samir Parikh[14], John Shapiro[14], Letizia De Chiara[15], Giulia Carangelo[15], Paola Romagnani[16,17], Sven Klussmann[18], Kai Hoehlig[18], Axel Vater[18] and Hans-Joachim Anders[1]

[1]Department of Medicine IV, Hospital of Ludwig-Maximilian-University, Munich, Germany; [2]Walther Straub-Institute of Pharmacology and Toxicology, Ludwig Maximilian University, Munich, Germany; [3]Division of Rheumatology, Endocrinology and Nephrology, Faculty of Medicine and Graduate School of Medicine, Hokkaido University, Sapporo, Japan; [4]Kunming Childen's Hospital, Yunnan, China; [5]Department of Urology, The Affiliated Hospital of Southwest Medical University, Luzhou, China; [6]Sichuan Clinical Research Center for Nephropathy, Luzhou, China; [7]School of Life Sciences, Nantong Laboratory of Development and Diseases, Nantong University, Nantong, China; [8]Institute for Cardiovascular Prevention (IPEK), Ludwig-Maximilians-Universität (LMU), Munich, Germany; [9]German Centre for Cardiovascular Research (DZHK), partner site Munich Heart Alliance, Munich, Germany; [10]Department of Biochemistry, Cardiovascular Research Institute Maastricht (CARIM), Maastricht University, Maastricht, The Netherlands; [11]Cluster for Nucleic Acid Therapeutics Munich (CNATM), Munich, Germany; [12]LaBooratory of Nephropathology, Institute of Pathology, RWTH Aachen University, Aachen, Germany; [13]Division of Nephrology and Clinical Immunology, RWTH Aachen University, Aachen, Germany; [14]Division of Nephrology, The Ohio State University Wexner Medical Center, Columbus, Ohio, USA; [15]Department of Biomedical, Experimental and Clinical Sciences "Mario Serio", University of Florence, Florence, Italy; [16]Department of Experimental and Biomedical Sciences "Mario Serio", University of Florence, Florence, Italy; [17]Nephrology and Dialysis Unit, Meyer Children's University Hospital, Florence, Italy; and [18]Aptarion biotech AG, Berlin, Germany

Cholesterol crystal embolism (CCE) implies immunothrombosis, tissue necrosis, and organ failure but no specific treatments are available. As CCE involves complement activation, we speculated that inhibitors of the C5a/C5aR axis would be sufficient to attenuate the consequences of CCE like that with systemic vasculitis. Cholesterol microcrystal injection into the kidney artery of wild-type mice initiated intra-kidney immunothrombosis within a few hours followed by a sudden drop of glomerular filtration rate and ischemic kidney necrosis after 24 hours. Genetic deficiency of either C3 or C5aR prevented immunothrombosis, glomerular filtration rate drop, and ischemic necrosis at 24 hours as did preemptive treatment with inhibitors of either C5a or C5aR. Delayed C5a blockade after crystal injection still resolved crystal clots and prevented all consequences. Thus, selective blockade of C5a or C5aR is sufficient to attenuate the consequences of established CCE and prospective inhibition in high-risk patients may be clinically feasible and safe.

Correspondence: *Hans-Joachim Anders, Medizinische Klinik und Poliklinik IV, Klinikum der Universität München, Ziemssenstr. 5, 80336 Munich, Germany. E-mail: hjanders@med.uni-muenchen.de*

Received 19 September 2023; revised 4 July 2024; accepted 19 July 2024

Kidney International (2024) ■, ■–■; https://doi.org/10.1016/j.kint.2024.07.020

KEYWORDS: acute kidney injury; crystals; infarct; necroinflammation; thrombosis

Translational Statement

Cholesterol crystal embolism (CCE) leads to immunothrombosis, ischemic necrosis, and organ dysfunction. Using a model of CCE, we demonstrate that selective inhibition of either complement factor 5a or its receptor C5aR is potent in preventing and resolving CCE-induced immunothrombosis and its consequences. C5a/C5aR inhibition early upon CCE or preemptively in high-risk patients should be clinically feasible and safe.

Cholesterol crystal embolism (CCE) is a potentially life-threatening complication of advanced atherosclerosis triggering microvascular thrombosis, ischemic tissue necrosis, and loss of organ function.[1] Kidney involvement in CCE is common and a predictor of poor outcomes.[1] Cholesterol crystals (CCs) trigger complement activation,[2] but the use of complement inhibitors in CCE has not been explored, partly because the reliable animal models were

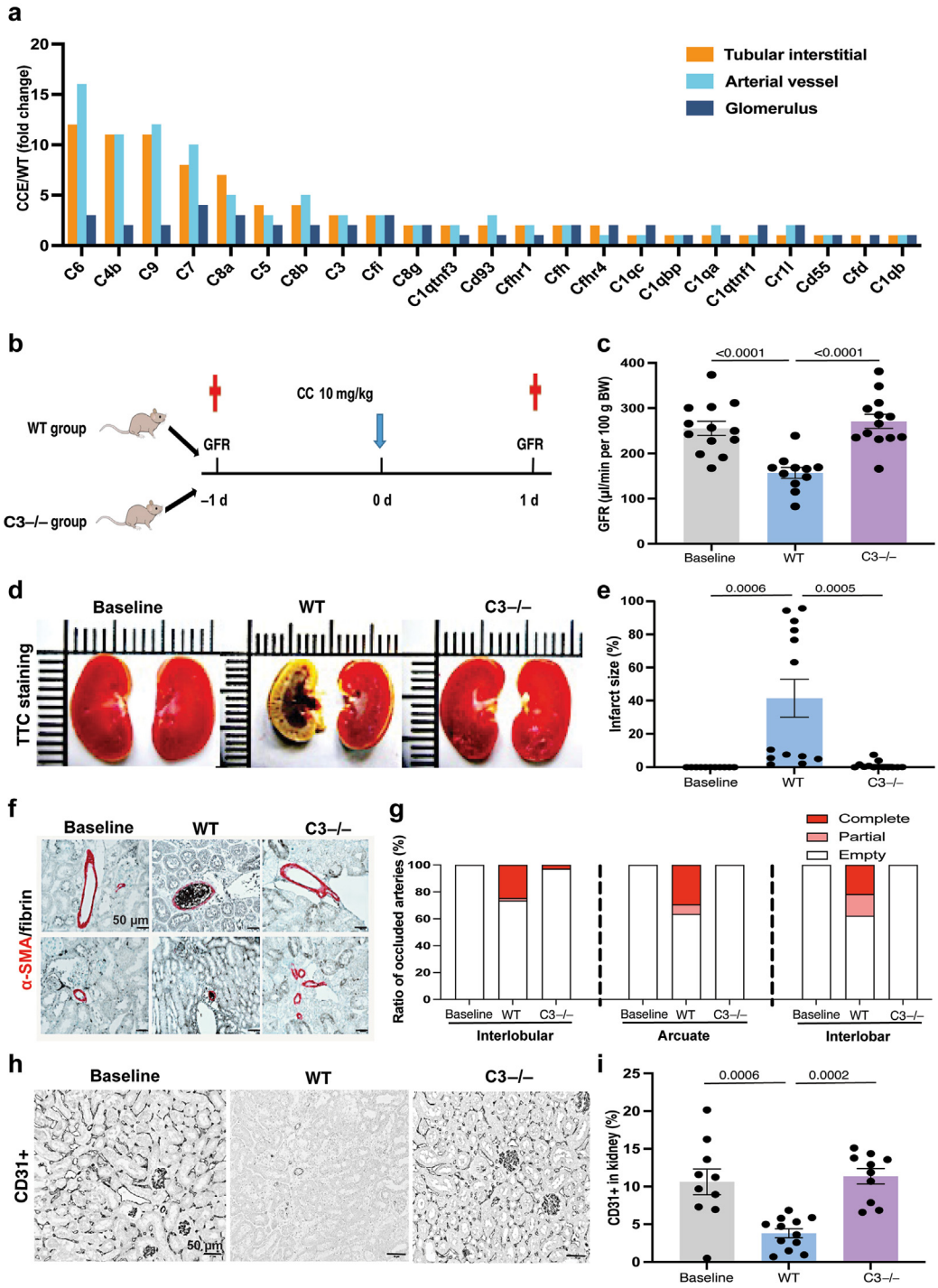

Figure 1 | C3 deficiency and cholesterol crystal embolism (CCE)–induced acute kidney injury. (**a**) Mass spectrometry for complement factors in different kidney compartments of the CCE model versus control. (**b**) Schematic of experimental design. (**c**) Baseline glomerular filtration rate (GFR) and GFR at 24 hours after intra-arterial injection of cholesterol crystals (CCs) into the left kidney artery of wild-type (WT) and C3-deficient (C3−/−) mice. (**d**) Representative images of 2,3,5-triphenyltetrazolium chloride (TTC) staining of kidney sections to distinguish viable from ischemic kidney tissue and to quantify infarct size. The red areas indicate living kidney tissue, and the white areas indicate infarcted kidney tissue. (**e**) Quantification of infarct size in WT and C3−/− mice. (**f**) Representative images of α-SMA (α-smooth muscle actin)/fibrin costaining. Fibrin-positive clots (black) in α-SMA+ arteries (red) indicate intravascular thrombosis in intrarenal arcuate and interlobular arterioles upon injection of phosphate-buffered saline or of CC in WT and C3−/− mice. (**g**) Ratio of occluded versus nonoccluded arteries in WT and C3−/− mice. Partial and complete vascular obstructions were quantified as percentage in all vessels of the available kidney sections. (**h**) Representative images of CD31 staining in WT and C3−/− mice. The back areas indicate CD31+. (**i**) Histological analysis upon microvascular staining for CD31 in WT and C3−/− mice. All quantitative data from 10 to 13 mice in each group are expressed as mean ± SEM. Bars = 50 μm. BW, body weight; C#, complement factor #. To optimize viewing of this image, please see the online version of this article at www.kidney-international.org.

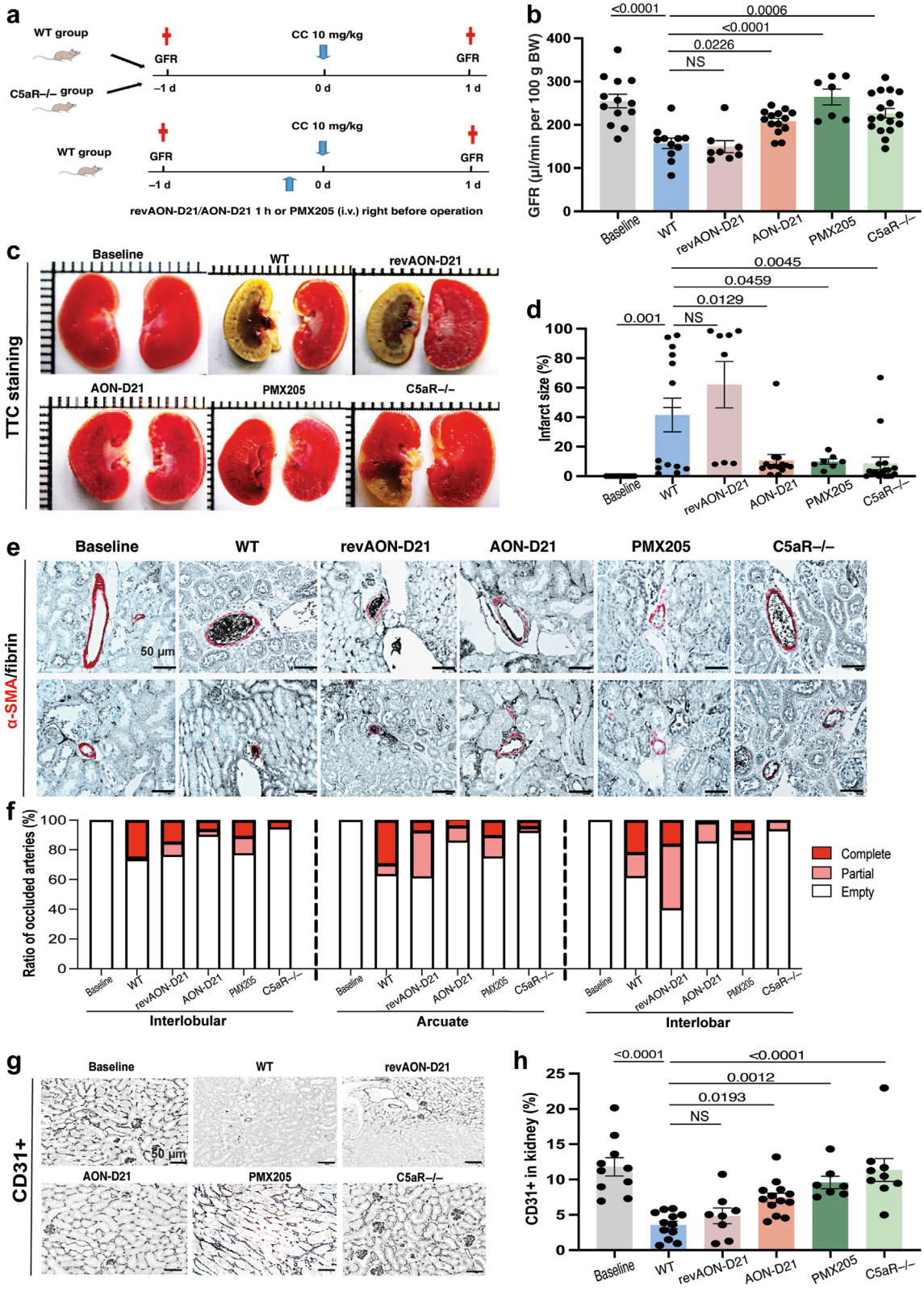

Figure 2 | Role of the complement factor 5a (C5a)/receptor of C5a (C5aR) axis in cholesterol crystal embolism–induced acute kidney injury. (**a**) Schematic of experimental design. (**b**) Baseline glomerular filtration rate (GFR) and at 24 hours after intra-arterial injection of cholesterol crystals (CCs) into the left kidney artery of wild-type (WT) and C5aR-deficient (C5aR−/−) mice or WT mice with a preemptive administration of the C5a-neutralizing L-aptamer AON-D21, the inactive control L-aptamer revAON-D21 consisting of the reverse sequences of AON-D21, or the C5aR antagonist PMX205. (**c**) Representative images of 2,3,5-triphenyltetrazolium chloride (TTC) staining of kidney sections to distinguish viable from ischemic kidney tissue and to quantify infarct size. The red areas indicate living kidney tissue, and the (continued)

not available. Recently, we developed a model of kidney CCE and discovered that not CCs alone but CC-induced microvascular thrombosis accounts for microvascular thrombosis, acute kidney injury (AKI), and ischemic infarction of the kidney.[3] Therefore, we explored the following 2 research hypotheses: (i) the complement system is a key mediator of CC-induced immunothrombosis, AKI, and ischemic kidney necrosis; and (ii) inhibition of complement factor 5a (C5a) or its receptor C5aR is sufficient to attenuate all consequences of CCE similar to its therapeutic effect in systemic vasculitis.

METHODS

Animal studies

Seven- to 8-week-old male healthy C57BL/6J, C3−/−, and C5aR−/− mice were obtained from the Jackson Laboratory. Group size calculation was based on the glomerular filtration rate (GFR) as a primary end point (SD = 26% of mean) and a power of 80% to detect an effect size of 20% at a 5% significance level.[3] All experimental procedures were approved by the local government authorities according to the European Directive 2010/63/EU. We induced experimental CCE by injecting CC into the left kidney artery and killed animals 24 hours later.[4,5] For space limitations, the detailed methods are provided in Supplementary Methods.

RESULTS AND DISCUSSION

Experimental CCE involves intravascular complement activation

To study the role of the complement system in CCE, we injected 10 mg/kg of CCs into the left kidney artery of mice and analyzed complement factors by using mass spectrometry (Figure 1a and b) and immunohistochemistry 24 hours later (Supplementary Figure S1A). Mass spectrometry revealed induction of the terminal complement pathway in the vascular and tubulointerstitial compartment and immunostaining localized C3c, C3d, C4d, complement factor H, and mannose-binding lectin to intra-arterial crystal clots.

C3 deficiency abrogates all consequences of CCE

CC injection caused a sudden drop of GFR on average by ∼40% within 24 hours of CC injection, that is, AKI (Figure 1c). The remaining 60% GFR is equivalent to 10% residual activity of the one kidney exposed to CCE. The contralateral kidney was left unaffected and contributed 50% to the GFR. 2,3,5-Triphenyltetrazolium chloride staining of kidney sections identified areas affected by ischemic infarction and allowed us to quantify infarct size compared to the unaffected contralateral kidney (Figure 1d and e). Immunostaining revealed thrombotic obstructions in smooth muscle actin–positive arcuate and interlobular arterial vessels by fibrin-positive clots surrounding CC clefts (Figure 1f and g) and loss of CD31+ endothelial cells as the cause of tissue infarction (Figure 1h and i). Kidney necrosis was associated with acute necroinflammation as indicated by the presence of neutrophils (Supplementary Figure S1B and C), cell death, and kidney injury all around and inside the ischemic necrosis area (Supplementary Figure S2D–F). Genetic deficiency of C3, a key element of all 3 complement activation pathways, entirely prevented crystal clot formation and any of the aforementioned consequences upon injection of the identical amount of CCs into the kidney artery (Figure 1c–i; Supplementary Figure S1B–G). These data are consistent with the known role of the complement system in immunothrombosis, including vascular thrombosis with microvascular injury triggered by other mechanisms, such as coronavirus disease 2019[6] or atypical hemolytic uremic syndrome. The latter provided the rationale for targeting C5, a downstream element of C3 activation fueling into C5a/C5aR-mediated immune cell recruitment and activation of immune cells as well as the formation of the membrane attack complex C5b-9.[7]

The C5a/C5aR axis critically mediates CCE-induced AKI

To investigate the contribution of the C5a/C5aR axis to CCE-induced AKI, we first induced identical CCE in mice with genetic deficiency of C5aR (Figure 2a) and obtained similar results as with C3 deficiency in terms of AKI, vascular thrombosis with microvascular injury, ischemic necrosis, CD31 loss in microvasculature, neutrophil infiltration, and kidney injury (Figure 2b–h; Supplementary Figure S2A–F). Next, we evaluated in wild-type mice the efficacy of AON-D21, an L-configured mixed RNA/DNA aptamer that binds and neutralizes murine C5a with favorable *in vivo* pharmacokinetics and pharmacodynamics regarding our study design.[8–10] Compared with the inactive control L-aptamer revAON-D21 consisting of the inverse sequence, the active inhibitor AON-D21 significantly attenuated all consequences of CCE as did the small molecule C5aR antagonist PMX205 (Figure 2b–f; Supplemenatry Figure S2A–F). PMX205, but not AON-D21, significantly preserved CD31+ endothelial cells from injury compared to untreated wild-type mice with CCE (Figure 2g and h). Thus, the C5a/C5aR axis seems to be the major effector element of intravascular complement

Figure 2 | (continued) white areas indicate infarcted kidney tissue. (**d**) Quantification of infarct size in WT and C5aR−/− or in WT mice with a preemptive administration of the C5a-neutralizing L-aptamer AON-D21, the inactive control L-aptamer revAON-D21 consisting of the reverse sequences of AON-D21, or the C5aR antagonist PMX205. (**e**) Representative images of α-SMA (α-smooth muscle actin)/fibrin costaining. Fibrin-positive clots (black) in α-SMA+ arteries (red) indicate intravascular thrombosis in intrarenal arcuate and interlobular arterioles upon injection of different treatments in WT mice and C5aR−/− mice. (**f**) Ratios of occluded versus nonoccluded arteries in WT mice with different treatments and C5aR−/− mice. Partial and complete vascular obstructions were quantified as percentage in all vessels of the available kidney sections. (**g**) Representative images of CD31 staining in WT mice with different treatments and C5aR−/− mice. The back areas indicate CD31+. (**h**) Histological analysis upon microvascular staining for CD31+ endothelial cells. No significant (NS) = $P > 0.05$. All quantitative data from 10 to 13 mice in each group are expressed as mean ± SEM. Bars = 50 μm. BW, body weight. To optimize viewing of this image, please see the online version of this article at www.kidney-international.org.

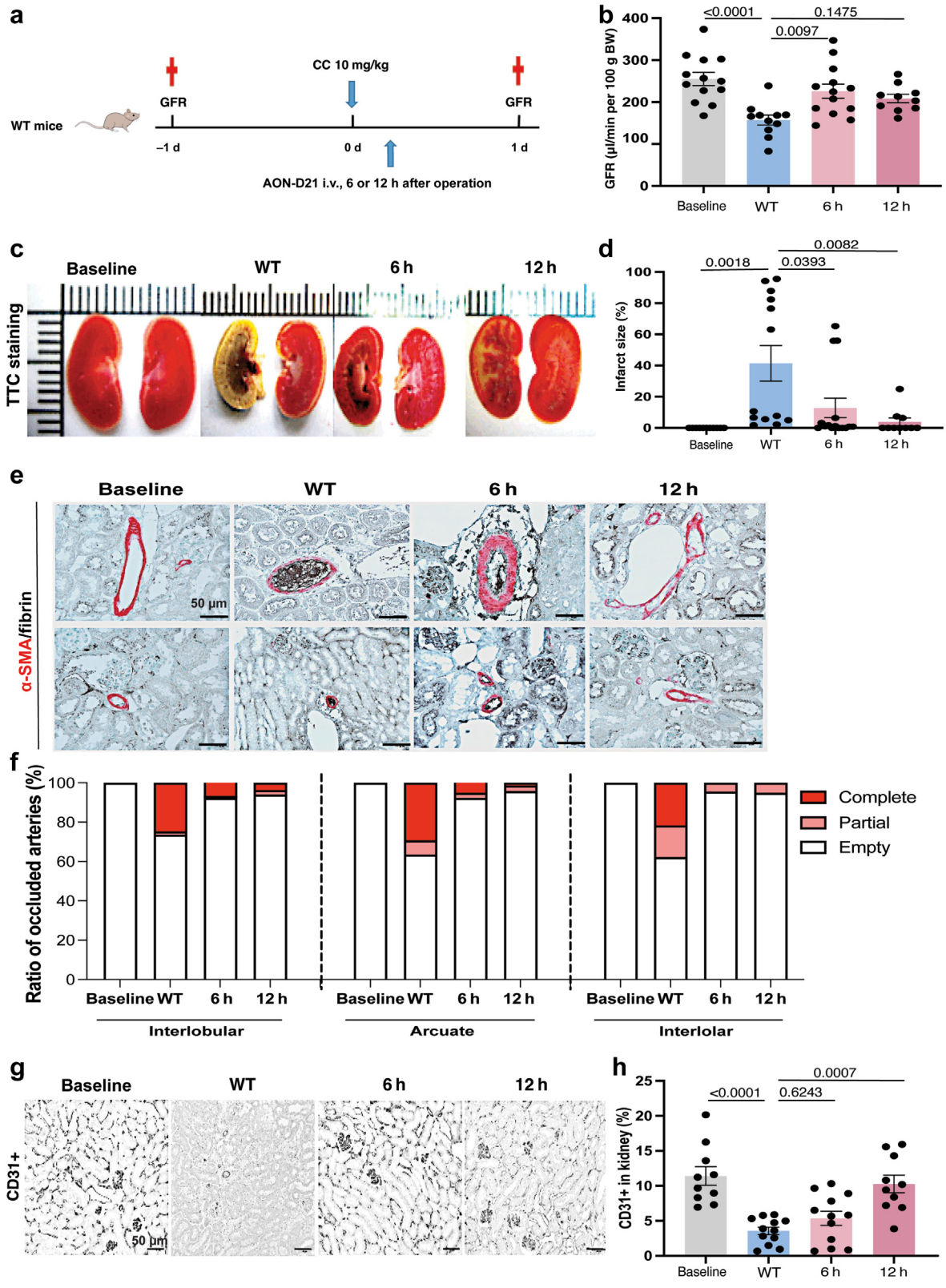

Figure 3 | Window of opportunity for complement factor 5a (C5a) inhibition in cholesterol crystal embolism–induced acute kidney injury. (**a**) Schematic of experimental design. (**b**) Baseline glomerular filtration rate (GFR) and at 24 hours after intra-arterial injection of cholesterol crystals (CCs) into the left kidney artery into wild-type (WT) mice with a single injection of the C5a inhibitor AON-D21 at different time points after CC injection as indicated. (**c**) Representative images of 2,3,5-triphenyltetrazolium chloride (TTC) staining of kidney sections to distinguish viable tissue from ischemic kidney tissue and to quantify infarct size. The red areas indicate living kidney tissue, and the white areas indicate infarcted kidney tissue. (**d**) Quantification of infarct size in WT mice with AON-D21 treatment at different time (continued)

activation upon CCE, which is consistent with data obtained from mouse models of anti-neutrophil cytoplasmic antibody vasculitis,[11,12] an autoimmune form of microvascular injury associated with complement-driven tissue necrosis.[13]

Mechanism of action of C5a inhibition

Single-cell RNA-sequencing analysis showed that complement factor transcripts are mostly absent in kidney parenchymal cells but C5aR is expressed by immune cells infiltrating the ischemic kidney (Supplementary Figure S3) and also in circulating platelets; thus, we assessed the impact of C5a inhibition on neutrophils and platelets *in vitro*. We evaluated neutrophils, which were the same in number in blood and bone marrow of C5aR-deficient (C5aR−/−) and wild-type mice (Supplementary Figure S4A–C). We tested their migratory capacity *in vitro* and found that C5aR deficiency abrogated neutrophil migration toward recombinant C5a and the inhibition of C5a in wild-type mice displayed similar results (Supplementary Figure S5A–D). Platelets are key components in arterial vascular thrombosis, thereby providing a thrombogenic surface for various circulating cells, including neutrophils. Therefore, we analyzed the role of C5aR in thrombus formation on the collagen-coated surface in the flow chamber. At a shear rate of 1000 s^{-1}, we observed impaired platelet adhesion and reduced thrombus formation on collagen matrix in C5aR−/− whole blood samples compared with wild-type samples (Supplementary Figure S6A and C), providing evidence for the antithrombotic potential of inhibiting C5aR function. Subsequently, we assessed the recruitment of neutrophils to previously formed thrombi under flow conditions. We observed that mouse neutrophils perfused through the system adhered to wild-type thrombi whereas the attachment of neutrophils to C5aR−/− thrombi was strongly inhibited (Supplementary Figure S6B and D), indicating that targeting C5aR during CCE reduces thrombus growth and prevents neutrophil adhesion to the formed thrombi. Together, these findings indicate that blockade of the C5a/C5aR axis effectively reduces the critical steps of vascular thrombosis with microvascular injury upon CCE, including the adhesion of platelets, thrombus growth, and migration and recruitment of neutrophils to the thrombogenic kidney injury sites.

C5a inhibition attenuates the consequences of established CCE

Vascular thrombus formation starts as early as 2 hours after CC injection, with first complete vascular occlusions at 6 hours and a plateau starting from 12 hours after CC injection.[4] We therefore tested the window of opportunity for C5a blockade with AON-D21 by administering the first dose either 6 or 12 hours after CC injection (Figure 3a). A 6-hour delayed initiation of AON-D21 therapy significantly attenuated GFR drop from baseline (Figure 3b). Infarct size was significantly reduced in both delayed treatment groups (Figure 3c and d), and these treatment groups also showed a potent attenuation of intravascular thrombotic lesions (Figure 3e and f). Furthermore, C5a inhibition starting at 12 hours after CC injection significantly prevented the loss of CD31+ endothelial cells (Figure 3g and h) and the influx of neutrophils (Supplementary Figure S7A and B), and reduced kidney injury and ischemic necrosis (Supplementary Figure S7C–F). We conclude that C5a inhibition with AON-D21 is sufficient to attenuate even established vascular occlusions after CCE, probably by shifting the balance between complement-driven prothrombotic activity and intrinsic fibrinolytic activity to the latter.[14]

These findings identify the C5a/C5aR axis as a selective complement target to prevent the consequences of CCE. The findings are somewhat unexpected because C3a, C3b, and C5b-9 were not expected to be redundant in this disease context. However, C5aR deficiency or inhibition was also potent in other animal models of kidney injury[11,12] and is proven to be profoundly therapeutic in human systemic vasculitis.[15,16] Indeed, renal vasculitis and CCE share immunothrombosis as an injurious pathomechanism.[13] Thrombosis results from a dysbalance of thrombogenesis and thrombolysis.[17] Thus, interfering with the key components of the complement system seems sufficient to tip the balance toward thrombolysis, which explains the profound effect of delayed intervention as well. The results between 6 and 12 hours after injection were not always consistent, which we attribute to the group size powered only to detect larger differences. Our results may pave the way for clinically feasible therapy of CCE, as the human C5aR inhibitor avacopan is on the market and safe in systemic vasculitis.[15] Limitations of this study include the lack of exploring later time points, but the enormous compensatory capacity of mouse kidney adaptation renders long-term follow-up of a unilateral model less informative. Altogether, C5a or C5aR is potent molecular therapeutic targets to resolve CCE-induced vascular thrombosis with microvascular injury, the key pathogenic element of CCE-related tissue injury and organ failure.

DISCLOSURE

AV, KH, and SK are employees of Aptarion. H-JA received research funds and consultancy fees from Aptarion. All the other authors declared no competing interests.

Figure 3 | (continued) points. (**e**) Representative images of α-SMA (α-smooth muscle actin)/fibrin costaining. Fibrin-positive clots (black) in α-SMA+ arteries (red) indicate intravascular thrombosis in intrarenal arcuate and interlobular arterioles. Size in WT mice with AON-D21 treatment at different time points. (**f**) Ratio of occluded versus nonoccluded arteries in WT mice with AON-D21 treatment at different time points. Partial and complete vascular obstructions were quantified as percentage in all vessels of the available kidney sections. (**g**) Representative images of CD31 staining in WT mice with AON-D21 treatment at different time points. (**h**) Histological analysis of microvascular staining for CD31 in WT mice with AON-D21 treatment at different time points. All quantitative data from 10 to 13 mice in each group are expressed as mean ± SEM. Bars = 50 μm. BW, body weight. To optimize viewing of this image, please see the online version of this article at www.kidney-international.org.

DATA STATEMENT

This study does not involve large data sets. The original data of the experiments will be shared upon reasonable request.

ACKNOWLEDGMENTS

The technical support of Yvonne Major, Uschi Kögelsperger, Jana Mandelbaum, and Anna Anfimiadou (all Division of Nephrology, Ludwig-Maximilians-Universität [LMU] Munich, Germany) is gratefully acknowledged.

FUNDING STATEMENT

This project was supported by the Deutsche Forschungsgemeinschaft (TRR332; projects A2, A7, B1, Z1, and AN372/20-2 and project ID 469035507). Experiments were performed using a Nikon Eclipse Ti2 microscope system (funded by DFG GZ:INST 86/1851-1 FUGG to Prof. Martha Merrow). PB was supported by the German Research Foundation (DFG; project IDs 322900939, 432698239, and 445703531), European Research Council (ERC Consolidator Grant No. 101001791), and the Federal Ministry of Education and Research (BMBF; STOP-FSGS-01GM2202C).

Supplementary material is available online at www.kidney-international.org.

REFERENCES

1. Scolari F, Ravani P. Atheroembolic renal disease. *Lancet*. 2010;375:1650–1660.
2. Nymo S, Niyonzima N, Espevik T, et al. Cholesterol crystal-induced endothelial cell activation is complement-dependent and mediated by TNF. *Immunobiology*. 2014;219:786–792.
3. Shi C, Kim T, Steiger S, et al. Crystal clots as therapeutic target in cholesterol crystal embolism. *Circ Res*. 2020;126:e37–e52.
4. Lyubenov L, Shi C, Zhao D, et al. Intravenous Glu-plasminogen attenuates cholesterol crystal embolism-induced thrombotic angiopathy, acute kidney injury and kidney infarction. *Nephrol Dial Transplant*. 2023;38:93–105.
5. Shi C, Zhao D, Lyubenov L, et al. Neutrophil circadian rhythm is associated with different outcomes of acute kidney injury due to cholesterol crystal embolism. *Front Cardiovasc Med*. 2022;9:974759.
6. Skendros P, Mitsios A, Chrysanthopoulou A, et al. Complement and tissue factor-enriched neutrophil extracellular traps are key drivers in COVID-19 immunothrombosis. *J Clin Invest*. 2020;130:6151–6157.
7. Mastellos DC, BGP Pires da Silva, Fonseca BAL, et al. Complement C3 vs C5 inhibition in severe COVID-19: early clinical findings reveal differential biological efficacy. *Clin Immunol*. 2020;220:108598.
8. Bujko K, Rzeszotek S, Hoehlig K, et al. Signaling of the complement cleavage product anaphylatoxin C5a through C5aR (CD88) contributes to pharmacological hematopoietic stem cell mobilization. *Stem Cell Rev Rep*. 2017;13:793–800.
9. Yatime L, Maasch C, Hoehlig K, et al. Structural basis for the targeting of complement anaphylatoxin C5a using a mixed l-RNA/l-DNA aptamer. *Nat Commun*. 2015;6:6481.
10. Hoehlig K, Maasch C, Shushakova N, et al. A novel C5a-neutralizing mirror-image (l-)aptamer prevents organ failure and improves survival in experimental sepsis. *Mol Ther*. 2013;21:2236–2246.
11. Dick J, Gan PY, Ford SL, et al. C5a receptor 1 promotes autoimmunity, neutrophil dysfunction and injury in experimental anti-myeloperoxidase glomerulonephritis. *Kidney Int*. 2018;93:615–625.
12. Schreiber A, Xiao H, Jennette JC, et al. C5a receptor mediates neutrophil activation and ANCA-induced glomerulonephritis. *J Am Soc Nephrol*. 2009;20:289–298.
13. Kitching AR, Anders HJ, Basu N, et al. ANCA-associated vasculitis. *Nat Rev Dis Primers*. 2020;6:71.
14. Schmidt CQ, Schrezenmeier H, Kavanagh D. Complement and the prothrombotic state. *Blood*. 2022;139:1954–1972.
15. Jayne DRW, Merkel PA, Schall TJ, et al. Avacopan for the treatment of ANCA-associated vasculitis. *N Engl J Med*. 2021;384:599–609.
16. Chalkia A, Flossmann O, Jones R, et al. Avacopan for ANCA-associated vasculitis with hypoxic pulmonary haemorrhage. *Nephrol Dial Transplant*. Publiushed online January 24, 2024. https://doi.org/10.1093/ndt/gfae020
17. Chang JC. Novel classification of thrombotic disorders based on molecular hemostasis and thrombogenesis producing primary and secondary phenotypes of thrombosis. *Biomedicines*. 2022;10:2706.